High- Q Magnetic Levitation and Control of Superconducting Microspheres at Millikelvin Temperatures

High-Q Magnetic Levitation and Control of Superconducting Microspheres at Millikelvin Temperatures

J. Hofer,[1,2,*] R. Gross,[3,4,5] G. Higgins,[2,6] H. Huebl,[3,4,5] O. F. Kieler,[7] R. Kleiner,[8] D. Koelle,[8] P. Schmidt,[2] J. A. Slater,[1,†] M. Trupke,[1] K. Uhl,[8] T. Weimann,[7] W. Wieczorek,[1,6] and M. Aspelmeyer[1,2]

[1]*Faculty of Physics, Vienna Center for Quantum Science and Technology (VCQ), University of Vienna, A-1090 Vienna, Austria*
[2]*Institute for Quantum Optics and Quantum Information (IQOQI), Austrian Academy of Sciences, A-1090 Vienna, Austria*
[3]*Walther-Meißner-Institut, Bayerische Akademie der Wissenschaften, D-85748 Garching, Germany*
[4]*Physik-Department, Technische Universität München, D-85748 Garching, Germany*
[5]*Munich Center for Quantum Science and Technology (MCQST), D-80799 München, Germany*
[6]*Department of Microtechnology and Nanoscience (MC2), Chalmers University of Technology, SE-412 96 Gothenburg, Sweden*
[7]*Physikalisch-Technische Bundesanstalt (PTB), D-38116 Braunschweig, Germany*
[8]*Physikalisches Institut, Center for Quantum Science (CQ) and LISA$^+$, University of Tuebingen, D-72076 Tuebingen, Germany*

(Received 6 December 2022; accepted 27 June 2023; published 25 July 2023)

We report the levitation of a superconducting lead-tin sphere with 100 μm diameter (corresponding to a mass of 5.6 μg) in a static magnetic trap formed by two coils in an anti-Helmholtz configuration, with adjustable resonance frequencies up to 240 Hz. The center-of-mass motion of the sphere is monitored magnetically using a dc superconducting quantum interference device as well as optically and exhibits quality factors of up to 2.6×10^7. We also demonstrate 3D magnetic feedback control of the motion of the sphere. The setup is housed in a dilution refrigerator operating at 15 mK. By implementing a cryogenic vibration isolation system, we can attenuate environmental vibrations at 200 Hz by approximately 7 orders of magnitude. The combination of low temperature, large mass, and high quality factor provides a promising platform for testing quantum physics in previously unexplored regimes with high mass and long coherence times.

DOI: 10.1103/PhysRevLett.131.043603

Diamagnets and superconductors partially expel magnetic fields, allowing stable levitation in field minima [1]. A prominent application of magnetically levitated systems is the use as ultraprecise acceleration sensors, most notably in the superconducting gravimeter [2], which relies on the levitation of centimeter-sized hollow superconducting spheres in a stable magnetic field generated by superconducting coils in persistent current mode. More recently, several proposals [3,4] have highlighted the potential of magnetic levitation for tests of quantum physics with macroscopic, micrometer-sized objects.

Successfully preparing a magnetically levitated particle in a quantum state requires a magnetic trap with low damping, low heating rates, and the ability to control the mechanical motion. Some of these features are already present in recent demonstrations of magnetically levitated systems, such as the levitation of permanent magnets above a superconducting surface [5,6] and the levitation of diamagnets in the field of permanent magnets at cryogenic temperatures [7] or room temperature [8]. However, as of yet, no system has combined these features. Furthermore, as typical levitation frequencies for these systems range from subhertz to kilohertz, the heating rate is dominated by environmental vibrations.

One of the most promising avenues toward the quantum regime is the levitation of a type-I (or zero-field-cooled type-II) superconductor in a magnetic field produced by persistent currents, as this avoids dissipation due to hysteresis and eddy currents, which is inherent to levitation schemes involving ferromagnets or flux-pinned type-II superconductors [9,10]. Using persistent currents should result in an extremely stable trap, as both the drift and noise can be kept extremely low [2,11,12]. Working at millikelvin temperatures also naturally enables coupling to nonlinear quantum systems such as superconducting qubits [3], and miniaturizing the trap architecture [13–15] might lead to fully on-chip coupled quantum systems [16]. In comparison with optical levitation, which has already been established as a means for studying massive objects in the quantum regime [17–19], magnetostatic levitation has the potential to access a new parameter regime of even larger mass [20,21] and longer coherence times [3,16]: While the size of optically levitated particles is, in practice, limited by

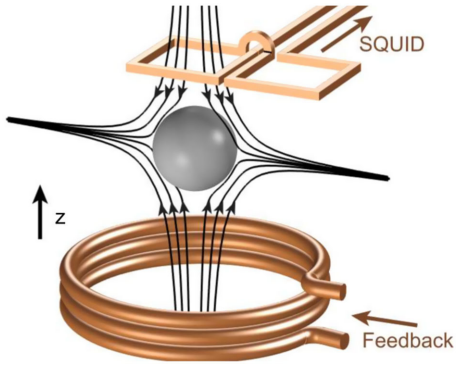

FIG. 1. Conceptual representation of the experiment showing the levitated sphere, the pickup coil, and the feedback coil. The trap field is depicted by its field lines.

the available laser power to the micrometer scale [22], magnetic levitation can support train-scale objects [23], and due to the static nature of the fields, there is no heating from photon absorption.

A first step toward a fully superconducting platform was presented in [24], where a lead particle was levitated in the magnetic field of a superconducting coil. This approach, however, was limited in performance by the presence of cryogenic exchange gas at 4 K and environmental vibrations. Here, we report an experiment that provides orders of magnitude improvements in both damping and vibration isolation. We demonstrate the levitation of a superconducting sphere in the magnetic field generated by a superconducting coil. We detect the center of mass (c.m.) motion of the particle magnetically by inductive coupling to a superconducting quantum interference device (SQUID) via a pickup coil (cf. Fig. 1) and demonstrate feedback control of all three c.m. translational degrees of freedom by real-time processing of the SQUID signal. We find that the motion of the particle has a low damping rate, corresponding to quality factors of up to 2.6×10^7. We also implement a custom vibration isolation system to reduce heating from environmental vibrations. Finally, we discuss the limitations of our current setup and the improvements that are necessary for ground state cooling.

Trapping.—The energy of an object of volume V with permeability μ in an applied magnetic field B_0 in free space can be approximated by $-1/2V(\mu - \mu_0)B_0^2$ [1], where μ_0 is the permeability of free space. Because $\nabla^2 B_0^2 \geq 0$, stable levitation is possible in a field minimum for $\mu < \mu_0$, i.e., for diamagnets. A superconducting sphere can act as a perfect diamagnet ($\mu = 0$), because it reacts to a change in the applied magnetic field by forming screening currents on its surface, counteracting the applied field and keeping the interior of the sphere field free.

For a sphere trapped in the field of an anti-Helmholtz coil, the resulting potential close to the field minimum is harmonic and two of the c.m. modes are degenerate [3,20]; to lift the degeneracy we use elliptical coils [25]. The z direction is along the coil axis, which coincides with the vertical direction, while x and y are perpendicular to z, with x along the major axis of the coils. We use numerical simulations [25] to model the magnetic field created by such an arrangement and confirm that the magnetic field near the center between the coils is well described by $(b_x x, b_y y, b_z z)$, where the field gradients b_i are proportional to the trap current with $|b_x| < |b_y| < |b_z|$ and $b_z = -(b_x + b_y)$. This field shape constitutes a three-dimensional harmonic trap for a levitated superconducting sphere with the c.m. frequencies [25]

$$f_i = \sqrt{\frac{3}{8\pi^2 \mu_0 \rho}} |b_i|, \tag{1}$$

where ρ is the density of the sphere.

Our setup is housed in a dilution refrigerator (Bluefors BF-LD400) with a loaded base temperature of approximately 15 mK. The microspheres are commercial (EasySpheres) solder balls with diameter 100(6) μm, made of a 90-10 lead-tin alloy with density $\rho = 10.9 \times 10^3$ kg/m^3. Lead-tin is a type-II superconductor with a critical temperature of approximately 7 K [37]. A single sphere is initially placed in a 3D-printed polylactide bowl glued to the lower trap coil, such that it rests around 1 mm below the trap center. The bowl helps to prevent accidental loss of the sphere during assembly and between measurement runs. After cooling down the system to millikelvin temperatures, lift-off is achieved by increasing the coil current until the upward magnetic force on the sphere is stronger than the downward gravitational and adhesive forces. The trap coils are surrounded by an aluminum shield with small openings for optical access and wires, which screens the sphere from magnetic field fluctuations when the aluminum is superconducting. To suppress field fluctuations from the trapping coils and feedback coil, we use a low pass filter and attenuation stages, respectively [25].

Readout.—A planar Niobium thin film gradiometric pickup coil consisting of two square loops positioned approximately 400 μm above the trap center is used to magnetically probe the particle motion. Each loop is 145 μm × 145 μm and the separation between the loops is 3 μm. As the particle moves, it induces a current in the pickup loop [25], which is connected with Nb wires to the input coil of a SQUID current sensor [38]. The SQUID has an intrinsic flux noise level of $S_\Phi^{1/2} = 0.8\ \mu\Phi_0/\sqrt{\text{Hz}}$, where $\Phi_0 \approx 2.1 \times 10^{-15}$ Wb is the flux quantum. When the SQUID is incorporated into the setup, and the pickup loop is connected, the noise rises to $S_\Phi^{1/2} \approx 10\ \mu\Phi_0/\sqrt{\text{Hz}}$. We believe this is due to external field fluctuations inductively coupling into the wires connecting the pickup loop and the SQUID. With a commercial SQUID (Supracon CSblue), that was used for some of the measurements, the noise floor in the setup further increased by an order of magnitude.

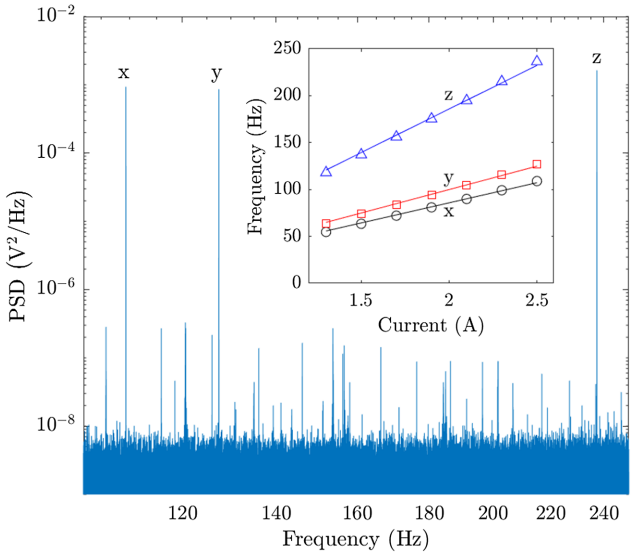

FIG. 2. The PSD of the SQUID signal displays three peaks which correspond to the c.m. modes of the particle. The motion of the particle is excited to approximately one micrometer rms displacement in this figure—measurement noise prevents us from resolving the equilibrium motion of the particle. The inset shows the linear dependence of the c.m. frequencies on the trap current. The solid lines are zero-intercept linear fits.

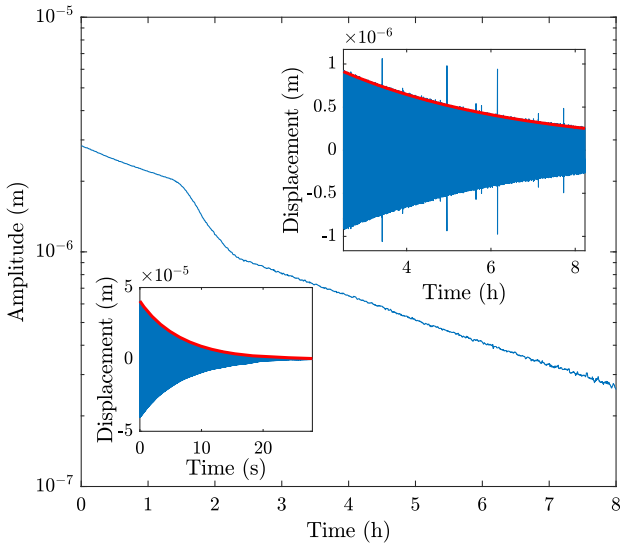

FIG. 3. Ringdown measurement of the z mode. The upper right inset shows a linear plot for the latter part of the data, starting at t = 2.5 h. The red line is a fit to an exponential decay. The spikes correspond to a brief loss of the SQUID lock, they were removed for the amplitude plot. The lower left inset shows a ringdown while direct feedback is applied (note that the x axis scale is in seconds).

To calibrate the SQUID signal, we optically record the motion of the sphere by illuminating it and imaging its shadow on a camera, while simultaneously recording the motion with the SQUID [25]. The coupling strengths (flux induced in the SQUID per sphere displacement) for the different motional modes depend on the position of the pickup loop in relation to the sphere as well as the trap gradients, i.e., mechanical frequencies. The highest measured coupling strength was approximately $13 \times 10^3\ \Phi_0/\mathrm{m}$ for the z mode and $3 \times 10^3\ \Phi_0/\mathrm{m}$ for the x and y modes. Together with a flux noise floor of $10\ \mu\Phi_0/\sqrt{\mathrm{Hz}}$ these coupling strengths correspond to a displacement sensitivity of approximately $1\ \mathrm{nm}/\sqrt{\mathrm{Hz}}$ for the z mode. During these measurements the separation between pickup loop and sphere was approximately 400 μm. We estimate that, with a smaller separation and an optimized pickup loop geometry, an improvement of 4 orders of magnitude is possible [25].

Mechanical frequencies.—The c.m. frequencies of the particle are visible in the power spectral density (PSD) of the SQUID signal, as shown in Fig. 2. The c.m. frequencies depend linearly on the magnetic field gradient of the trap [see Eq. (1)] and, thus, the current in the trap coils, as shown in the inset. The highest frequency reached in the present setup is 240 Hz (corresponding to $b_z \approx 150\ \mathrm{T/m}$), limited by the maximum current output of the low-noise current source. We can trap at lower frequencies, down to $f_z \approx 20$ Hz, where the lower limit stems from the gravity-induced shift of the trapping position and our trap geometry. However, at low trapping frequencies, the sphere is strongly excited by environmental vibrations.

We can apply a magnetic feedback force on the levitated sphere by processing the SQUID signal on an FPGA (STEMlab 125-14) and applying a feedback current to a small coil with approximately 20 windings positioned approximately 1 mm below the trap center [25]. As measurement noise prevents us from resolving the equilibrium c.m. motion of the particle, we use feedback here only as a means to quickly adjust the amplitudes and prepare other measurements (cf. Fig. 3, inset).

Quality factor.—We measure the quality factor by performing ringdown measurements, where the initial starting amplitude is set by applying an appropriate feedback signal before the start of the measurement. We do see occasional jumps in the damping rate (cf. Fig. 3), which we attribute to the detaching and attaching of flux lines to a pinning center. Unpinned flux lines can move within the superconductor (flux creep), a mechanism that is known to cause damping in the levitation of flux-pinned superconductors or magnets [10,39]. Although we do not apply a magnetic field during the cooldown, there is a nonzero background field, and hence, we expect some frozen-in flux to be present in the levitated sphere. As a consequence, the measured quality factors vary with time and between measurement runs, but they are generally between 1×10^7 and 2.5×10^7 for the z mode and about half as high for the x and y modes. The highest quality factor we have measured is 2.6×10^7 at 212 Hz, corresponding to a dissipation rate of $5 \times 10^{-5}\ \mathrm{s}^{-1}$, and likely still limited by flux creep inside the particle. We also consider other possible contributions to the damping [25], but find that the

expected contributions cannot explain the measured values. In future experiments, we plan to use a particle made of a type-I superconductor such as monocrystalline lead, which will expel all magnetic flux via the Meissner effect and prevent flux creep.

Sensing.—A massive system acting as a harmonic oscillator can be used for force and acceleration sensing, with the sensitivities depending on the mass m and the dissipation rate γ of the oscillator. In equilibrium with a thermal bath at temperature T_0, the thermal force noise is given by $\sqrt{S_{FF}^{\mathrm{th}}} = \sqrt{4k_B T_0 m\gamma}$ [40], where k_B is Boltzmann's constant. The dissipation rate γ is related to the quality factor Q and the angular mechanical resonance frequency ω_0 by $\gamma = \omega_0/Q$. The corresponding acceleration sensitivity is $\sqrt{S_{FF}^{\mathrm{th}}}/m$. For a particle of mass $m \approx 5.6$ μg, assuming it is in thermal equilibrium with its surroundings in the dilution refrigerator at 15 mK, this sets the limits for force and acceleration sensing at 5×10^{-19} N/$\sqrt{\mathrm{Hz}}$ and 9×10^{-12} g/$\sqrt{\mathrm{Hz}}$, using our highest measured quality factor $Q = 2.6 \times 10^7$ at 212 Hz. Our current experimental sensitivities are approximately 1 order of magnitude above the thermal noise, limited by drifts in the trap current and measurement noise [25].

Cryogenic vibration isolation.—Vibrations of the cryostat accelerate the trapping coils and, thus, the trap center, effecting a force onto the levitated sphere. Denoting the vibrational PSD by $S_{\epsilon\epsilon}$, the displacement PSD of our sphere becomes $|\chi(\omega)|^2 m^2 \omega_0^4 S_{\epsilon\epsilon}(\omega)$, where χ denotes the mechanical susceptibility. From independent accelerometer measurements on the cryostat, we estimate $\sqrt{S_{\epsilon\epsilon}} \approx 1 \times 10^{-10}$ m/$\sqrt{\mathrm{Hz}}$ at 200 Hz, which would result in a peak height of 2.6×10^{-3} m/$\sqrt{\mathrm{Hz}}$ and a root-mean-square displacement of 9 μm, corresponding to an effective temperature of 6×10^{10} K. To mitigate the effects of vibrations, we implement a passive cryogenic vibration isolation system: the aluminum shield containing the trap is hung from the 4 K stage of the dilution refrigerator via 38 μm-thick stainless steel wires and two intermediate stages. The system acts like a triple pendulum, offering isolation from horizontal (x and y) vibrations, while the elasticity of the wires provides isolation from vertical (z) vibrations. To prevent coupling of external vibrations into the experimental setup via electrical wires and the copper braids used for thermalization, we connect these wires and braids to an additional vibration isolation platform, as represented in Fig. 4. Vibrations of the experimental system could also be induced by fluctuating magnetic fields acting on the aluminum shield. To prevent this, we surround the setup by a second aluminum shield which is rigidly mounted to the cryostat. We typically operate at vertical (z) trap frequencies above 200 Hz and initially found that the vibration isolation system attenuates vibrations at these frequencies by approximately 5 orders of magnitude. We have further improved the system by optimizing the mass and wire length for each stage, leading to an attenuation of almost 7 orders of magnitude at 200 Hz. Theoretically, vibrations along the horizontal axis as well as librational fluctuations around the axes are suppressed even more, but in practice, we expect vibrations from the vertical axis to couple into all degrees of freedom [41]. More details on the vibration isolation platform are provided in [25].

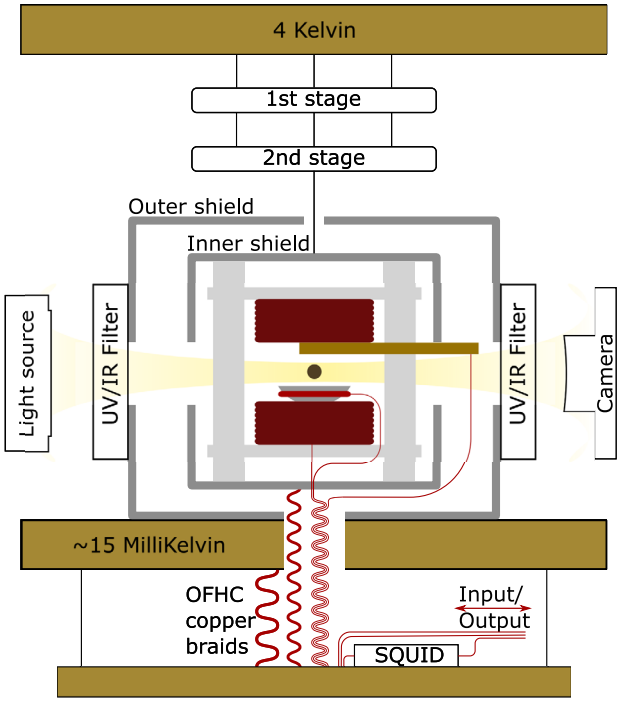

FIG. 4. Sketch of the setup including the vibration isolation system (not to scale). The light source is turned on only for calibration measurements. The UV-IR cutoff filters on the millikelvin stage prevent ambient radiation from heating the levitated sphere. Thermal connections are made with oxygen free high conductivity (OFHC) copper braids.

Prospects for ground state cooling.—Now, we discuss the potential of this system to reach the ground state, which would be a first step toward accessing the quantum regime. SQUID noise can be separated into flux noise $S_{\phi\phi}$ and noise in the circulating current S_{JJ}, which may be partially correlated [42] and fulfill $\sqrt{S_{\phi\phi}S_{JJ} - S_{\phi J}^2} \geq \hbar$ [43,44]. The flux noise results in the measurement noise $(S_{\phi\phi}/\eta^2)$, while the current noise corresponds to a back action $\eta^2 S_{JJ}$, where η is the coupling strength. Applying direct feedback with optimum gain and assuming vanishing correlations between flux and current noise, one can estimate the final phonon occupation [25] as

$$\bar{n} = \frac{1}{\hbar\eta^2}(k_B T_0 m\gamma \widetilde{L_S}) + \frac{1}{2}\left(\frac{\sqrt{S_{\phi\phi}S_{JJ}}}{\hbar} - 1\right),$$

where $\widetilde{L_S} = \sqrt{(S_{\phi\phi}/S_{JJ})}$ depends on the working point of the SQUID and is typically on the order of the SQUID

inductance L_S. The first term describes heating from coupling to an effective thermal reservoir with temperature T_0, while the second term is the backaction limit under continuous feedback. We can reach a coupling strength of $\eta \approx 5.5 \times 10^7\ \Phi_0/\mathrm{m}$ [25], so assuming $T_0 \approx 15$ mK and a typical SQUID inductance of $L_S \approx 15$ pH, we need $\gamma \approx 1 \times 10^{-6}\ \mathrm{s}^{-1}$ to keep the former negligible. Ground state cooling then requires $\sqrt{S_{\phi\phi} S_{JJ}} < 3\hbar$. In addition to feedback cooling with a SQUID, we will investigate other potential avenues for ground state cooling such as coupling the levitated sphere to a flux qubit or a microwave cavity [3,45–47].

Discussion and outlook.—We built a platform based on the diamagnetic levitation of a superconductor in a magnetostatic trap in a dilution refrigerator at 15 mK and demonstrate quality factors exceeding 1×10^7 for the three c.m. modes of a 5.6 μg oscillator. The high quality factors result in excellent sensing capabilities, with achievable force (acceleration) sensitivities that are, otherwise, only reached with much smaller (larger) masses [2,48]. We also demonstrated simultaneous feedback cooling of all c.m. modes using either direct or parametric feedback. While we have focused, here, on a 100 μm-sized sphere, the setup allows for particles from submicron size to millimeter size to be levitated [20]. We have identified improvements to mitigate technical issues: First, we plan to use a type-I superconducting sphere to avoid trapped flux and dissipation caused by flux creep, which we expect is limiting our quality factor. Second, we can improve the magnetomechanical coupling by 4 orders of magnitude by better positioning of the pickup coil and by using a pickup coil with multiple windings matched to the input coil of the SQUID. Together with an optimized SQUID shielded from environmental noise (such that our readout is limited by the intrinsic SQUID noise), this would result in an improvement of the measurement noise floor by 6 orders of magnitude [25]. Third, we plan to implement a persistent current switch to improve the trap current stability. With these improvements, our system offers a promising approach for bringing microgram objects to the quantum regime, which opens a potential avenue for quantum-limited acceleration sensing or even probing quantum effects of gravity [49–52].

The data of this study are available at the Zenodo repository [53].

We thank G. Kirchmair, O. Romero-Isart, and A. Sanchez for discussions. We thank Matthias Rudolph for assisting with the initial setup of a SQUID measurement system. We thank F. Wulschner for setting up a helium flow cryostat and assisting with measurements during the initial phase of the project. This work was supported by the European Union's Horizon 2020 research and innovation programme under Grant Agreement No. 863132 (iQLev), the European Union's Horizon Europe 2021–2027 Framework Programme under Grant Agreement No. 101080143 (SuperMeQ), the European Research Council (ERC CoG QLev4G and ERC Synergy QXtreme), and the Austrian Science Fund (FWF) under Project No. F40 (SFB FOQUS). We gratefully acknowledge financial support from the Deutsche Forschungsgemeinschaft (DFG, German Research Foundation) under Germany's Excellence Strategy Grant No. EXC-2111–390814868. G. H. acknowledges support from the Swedish Research Council (Grant No. 2020-00381). P. S. is supported by the Alexander von Humboldt Foundation through a Feodor Lynen Fellowship.

*joachim.hofer@univie.ac.at
†Present address: QuTech, Delft University of Technology, Delft, The Netherlands.

[1] E. H. Brandt, Levitation in physics, Science **243**, 349 (1989).
[2] J. M. Goodkind, The superconducting gravimeter, Rev. Sci. Instrum. **70**, 4131 (1999).
[3] O. Romero-Isart, L. Clemente, C. Navau, A. Sanchez, and J. I. Cirac, Quantum Magnetomechanics with Levitating Superconducting Microspheres, Phys. Rev. Lett. **109**, 147205 (2012).
[4] M. Cirio, G. K. Brennen, and J. Twamley, Quantum Magnetomechanics: Ultrahigh-Q-Levitated Mechanical Oscillators, Phys. Rev. Lett. **109**, 147206 (2012).
[5] A. Vinante, P. Falferi, G. Gasbarri, A. Setter, C. Timberlake, and H. Ulbricht, Ultralow Mechanical Damping with Meissner-Levitated Ferromagnetic Microparticles, Phys. Rev. Appl. **13**, 064027 (2020).
[6] J. Gieseler, A. Kabcenell, E. Rosenfeld, J. D. Schaefer, A. Safira, M. J. A. Schuetz, C. Gonzalez-Ballestero, C. C. Rusconi, O. Romero-Isart, and M. D. Lukin, Single-Spin Magnetomechanics with Levitated Micromagnets, Phys. Rev. Lett. **124**, 163604 (2020).
[7] Y. Leng, R. Li, X. Kong, H. Xie, D. Zheng, P. Yin, F. Xiong, T. Wu, C.-K. Duan, Y. Du, Z.-q. Yin, P. Huang, and J. Du, Mechanical Dissipation Below 1 μHz with a Cryogenic Diamagnetic Levitated Micro-Oscillator, Phys. Rev. Appl. **15**, 024061 (2021).
[8] C. W. Lewandowski, T. D. Knowles, Z. B. Etienne, and B. D'Urso, High-Sensitivity Accelerometry with a Feedback-Cooled Magnetically Levitated Microsphere, Phys. Rev. Appl. **15**, 014050 (2021).
[9] T. Wang, S. Lourette, S. R. O'Kelley, M. Kayci, Y. B. Band, Derek F. Jackson Kimball, A. O. Sushkov, and D. Budker, Dynamics of a Ferromagnetic Particle Levitated Over a Superconductor, Phys. Rev. Appl. **11**, 044041 (2019).
[10] E. H. Brandt, Friction in levitated superconductors, Appl. Phys. Lett. **53**, 1554 (1988).
[11] R. S. Van Dyck, D. L. Farnham, S. L. Zafonte, and P. B. Schwinberg, Ultrastable superconducting magnet system for a penning trap mass spectrometer, Rev. Sci. Instrum. **70**, 1665 (1999).
[12] J. W. Britton, J. G. Bohnet, B. C. Sawyer, H. Uys, M. J. Biercuk, and J. J. Bollinger, Vibration-induced field fluctuations in a superconducting magnet, Phys. Rev. A **93**, 062511 (2016).

[13] M. G. Latorre, J. Hofer, M. Rudolph, and W. Wieczorek, Chip-based superconducting traps for levitation of micrometer-sized particles in the Meissner state, Supercond. Sci. Technol. **33**, 105002 (2020).
[14] M. G. Latorre, A. Paradkar, D. Hambraeus, G. Higgins, and W. Wieczorek, A chip-based superconducting magnetic trap for levitating superconducting microparticles, IEEE Trans. Appl. Supercond. **32**, 1 (2022).
[15] M. Gutierrez Latorre, G. Higgins, A. Paradkar, T. Bauch, and W. Wieczorek, Superconducting Microsphere Magnetically Levitated in an Anharmonic Potential with Integrated Magnetic Readout, Phys. Rev. Appl. **19**, 054047 (2023).
[16] H. Pino, J. Prat-Camps, K. Sinha, B. P. Venkatesh, and O. Romero-Isart, On-chip quantum interference of a superconducting microsphere, Quantum Sci. Technol. **3**, 025001 (2018).
[17] U. Delic, M. Reisenbauer, K. Dare, D. Grass, Vuletic Vladan, N. Kiesel, and M. Aspelmeyer, Cooling of a levitated nanoparticle to the motional quantum ground state, Science **367**, 892 (2020).
[18] L. Magrini, P. Rosenzweig, C. Bach, A. Deutschmann-Olek, S. G. Hofer, S. Hong, N. Kiesel, A. Kugi, and M. Aspelmeyer, Real-time optimal quantum control of mechanical motion at room temperature, Nature (London) **595**, 373 (2021).
[19] F. Tebbenjohanns, M. L. Mattana, M. Rossi, M. Frimmer, and L. Novotny, Quantum control of a nanoparticle optically levitated in cryogenic free space, Nature (London) **595**, 378 (2021).
[20] J. Hofer and M. Aspelmeyer, Analytic solutions to the Maxwell–London equations and levitation force for a superconducting sphere in a quadrupole field, Phys. Scr. **94**, 125508 (2019).
[21] C. Navau, S. Minniberger, M. Trupke, and A. Sanchez, Levitation of superconducting microrings for quantum magnetomechanics, Phys. Rev. B **103**, 174436 (2021).
[22] F. Monteiro, S. Ghosh, A. G. Fine, and D. C. Moore, Optical levitation of 10-ng spheres with nano-g acceleration sensitivity, Phys. Rev. A **96**, 063841 (2017).
[23] Francis C. Moon and P.-Z. Chang, *Superconducting Levitation: Applications to Bearings and Magnetic Transportation* (Wiley-VCH, New York, 1995).
[24] B. van Waarde, The lead zeppelin: A force sensor without a handle, Ph.D. thesis, Leiden University, 2016.
[25] See Supplemental Material at http://link.aps.org/supplemental/10.1103/PhysRevLett.131.043603 for more information on the derivation of trap parameters, the effects of trap current fluctuations, the vibration isolation system, estimations of different contributions to the damping, the calibration of the SQUID signal, as well as more details on ground state cooling, which includes Refs. [26–36].
[26] L. Neuhaus, R. Metzdorff, S. Chua, T. Jacqmin, T. Briant, A. Heidmann, P.-F. Cohadon, and S. Deléglise, PyRPL (Python Red Pitaya Lockbox)—An open-source software package for FPGA-controlled quantum optics experiments, in *Proceedings of the 2017 Conference on Lasers and Electro-Optics Europe European Quantum Electronics Conference (CLEO/Europe-EQEC)* (IEEE, New York, 2017), p. 1.
[27] L. D. Hinkle and B. R. F. Kendall, Pressure-dependent damping of a particle levitated in vacuum, J. Vac. Sci. Technol. A **8**, 2802 (1990).
[28] J. M. Martinis and J. Clarke, Signal and noise theory for a dc SQUID amplifier, J. Low Temp. Phys. **61**, 227 (1985).
[29] J. C. Crocker and D. G. Grier, Methods of digital video microscopy for colloidal studies, J. Colloid Interface Sci. **179**, 298 (1996).
[30] D. D. Awschalom, J. R. Rozen, M. B. Ketchen, W. J. Gallagher, A. W. Kleinsasser, R. L. Sandstrom, and B. Bumble, Low-noise modular microsusceptometer using nearly quantum limited dc SQUIDs, Appl. Phys. Lett. **53**, 2108 (1988).
[31] P. Carelli, M. G. Castellano, G. Torrioli, and R. Leoni, Low noise multiwasher superconducting interferometer, Appl. Phys. Lett. **72**, 115 (1998).
[32] H. Wheeler, Simple inductance formulas for radio coils, Proc. Inst. Radio Eng. **16**, 1398 (1928).
[33] T. W. Penny, A. Pontin, and P. F. Barker, Performance and limits of feedback cooling methods for levitated oscillators: A direct comparison, Phys. Rev. A **104**, 023502 (2021).
[34] J. Martinis and J. Clarke, Measurements of current noise in dc SQUIDS, IEEE Trans. Magn. **19**, 446 (1983).
[35] P. Falferi, M. Bonaldi, M. Cerdonio, R. Mezzena, G. A. Prodi, A. Vinante, and S. Vitale, $10\hbar$ superconducting quantum interference device amplifier for acoustic gravitational wave detectors, Appl. Phys. Lett. **93**, 172506 (2008).
[36] M. E. Gehm, K. M. O'Hara, T. A. Savard, and J. E. Thomas, Dynamics of noise-induced heating in atom traps, Phys. Rev. A **58**, 3914 (1998).
[37] J. D. Livingston, Magnetic properties of superconducting lead-base alloys, Phys. Rev. **129**, 1943 (1963).
[38] J.-H. Storm, O. Kieler, and R. Körber, Towards ultrasensitive SQUIDs based on submicrometer-sized Josephson junctions, IEEE Trans. Appl. Supercond. **30**, 1 (2020).
[39] V. V. Nemoshkalenko, E. H. Brandt, A. A. Kordyuk, and B. G. Nikitin, Dynamics of a permanent magnet levitating above a high-T_c superconductor, Physica (Amsterdam) **170C**, 481 (1990).
[40] R. Kubo, The fluctuation-dissipation theorem, Rep. Prog. Phys. **29**, 255 (1966).
[41] T. L. Aldcroft, P. F. Michelson, R. C. Taber, and F. A. McLoughlin, Six-degree-of-freedom vibration isolation systems with application to resonant-mass gravitational radiation detectors, Rev. Sci. Instrum. **63**, 3815 (1992).
[42] C. D. Tesche and J. Clarke, dc SQUID: Current noise, J. Low Temp. Phys. **37**, 397 (1979).
[43] R. H. Koch, D. J. Van Harlingen, and J. Clarke, Quantum noise theory for the dc SQUID, Appl. Phys. Lett. **38**, 380 (1981).
[44] V. Danilov, K. Likharev, and A. Zorin, Quantum noise in squids, IEEE Trans. Magn. **19**, 572 (1983).
[45] P. Schmidt, M. T. Amawi, S. Pogorzalek, F. Deppe, A. Marx, R. Gross, and H. Huebl, Sideband-resolved resonator electromechanics based on a nonlinear Josephson inductance probed on the single-photon level, Commun. Phys. **3**, 233 (2020).
[46] O. Shevchuk, G. A. Steele, and Y. M. Blanter, Strong and tunable couplings in flux-mediated optomechanics, Phys. Rev. B **96**, 014508 (2017).

[47] D. Zoepfl, M. L. Juan, C. M. F. Schneider, and G. Kirchmair, Single-Photon Cooling in Microwave Magnetomechanics, Phys. Rev. Lett. **125**, 023601 (2020).

[48] D. Hempston, J. Vovrosh, M. Toroš, G. Winstone, M. Rashid, and H. Ulbricht, Force sensing with an optically levitated charged nanoparticle, Appl. Phys. Lett. **111**, 133111 (2017).

[49] S. P. Kumar and M. B. Plenio, On quantum gravity tests with composite particles, Nat. Commun. **11**, 3900 (2020).

[50] C. Marletto and V. Vedral, Gravitationally Induced Entanglement Between Two Massive Particles is Sufficient Evidence of Quantum Effects in Gravity, Phys. Rev. Lett. **119**, 240402 (2017).

[51] S. Bose, A. Mazumdar, G. W. Morley, H. Ulbricht, M. Toroš, M. Paternostro, A. A. Geraci, P. F. Barker, M. S. Kim, and G. Milburn, Spin Entanglement Witness for Quantum Gravity, Phys. Rev. Lett. **119**, 240401 (2017).

[52] M. Aspelmeyer, How to avoid the appearance of a classical world in gravity experiments, arXiv:2203.05587.

[53] J. Hofer *et al.*, Data Used in the Article "High-Q Magnetic Levitation and Control of Superconducting Microspheres at Millikelvin Temperatures", Zenodo, 10.5281/zenodo.7837944 (2023).